Crystal structure of Eu-doped magnetoplumbite-type lanthanum aluminum oxynitride with emission site splitting.

Yuji Masubuchi*, Tomoyuki Hata, Teruki Motohashi and Shinichi Kikkawa

Affiliations:

Faculty of Engineering, Hokkaido University, N13 W8, Kita-ku, Sapporo 060-8628, Japan

*Corresponding author: Y. Masubuchi; address: Faculty of Engineering, Hokkaido University, Sapporo 060-8628, Japan; Tel/Fax: +81-(0)11-706-6742/6740; E-mail: yuji-mas@eng.hokudai.ac.jp

Abstract

Eu-doped lanthanum aluminum oxynitride ($LaAl_{12}(O,N)_{19}$) with magnetoplumbite structure was prepared by nitridation of the oxide precursor obtained from aluminum glycine gel and subsequent post-annealing. Eu-doped lanthanum aluminum oxynitride exhibited blue light emission at 440 nm with a shoulder at 464 nm under excitation at 254 nm. Isostructural Eu-doped calcium aluminum oxide ($CaAl_{12}O_{19}$) exhibited a single emission peak at 415 nm. Structural refinement using neutron powder diffraction indicated that the lanthanum site occupied partially by Eu^{2+} splits into 2*d* and 6*h* sites in the aluminum oxynitride. The longer emission and the shoulder peak in the former aluminum oxynitride were observed in relation to the increasing covalency as well as crystal field splitting around doped Eu^{2+} induced by site splitting involved with the two kinds of anions.

Keywords

Lanthanum aluminum oxynitride; Magnetoplumbite structure; Photoluminescence; Neutron diffraction.

1. Introduction

White light emitting diodes (LEDs) have received much attention as high efficiency, safe and environmentally friendly devices [1,2]. In white LED applications, blue LED light is combined with yellow light emitted from a phosphor to obtain white light [3]. Both green and red light emitting phosphors have been used in appropriate amounts with yellow phosphor to improve the color rendering properties of white LEDs. These phosphorous materials have been developed among SiAlON related compounds that have excellent color rendering indexes. However, the luminescence efficiency of white LEDs is low due to the strong reabsorption of blue light by the red and green phosphors [4,5]. In white LEDs with multiple phosphor components, the color balance must be controlled. Recently, single component phosphors that exhibit multiple color emission have emerged to overcome those problems. Multiple emissions have been obtained for Eu and Mn co-doped full color phosphors [6,7]. Multi-color emission has been also reported for several phosphors doped with only Eu^{2+} [8,9], where several crystallographic sites in their host structure were simultaneously substituted by Eu^{2+}. Kikkawa et al. reported three emission peaks at 400, 475 and 520 nm for Eu^{2+}-doped AlON with an impurity phase of magnetoplumbite (MP)-type $EuAl_{12}O_{19}$ [10]. They attributed the multiple emissions to the presence of the different coordination environments around Eu^{2+} with different O^{2-}/N^{3-} ratios in the MP structure.

MP-type alkaline earth (AE) aluminum oxide ($AEAl_{12}O_{19}$) and aluminum oxide with β-alumina structure have been investigated to obtain phosphors doped with Eu^{2+} [11,12]. Both structures belong to the same space group ($P6_3/mmc$) and are constructed of spinel blocks and intermediate layers. Large cations such as Ba^{2+} occupy the nine-fold coordination sites in the intermediate layer of the β-alumina structure. Small cations, such as Sr^{2+} or Ca^{2+}, are located in the twelve coordination sites of the MP structure in aluminum oxide [13,14]. A Eu-doped compound was also prepared using barium aluminum oxynitride with β-alumina structure and its emission efficiency was compared with aluminum oxide [15]. The MP structure has been reported only in lanthanum aluminum oxynitride [16-18]. However, to the best of our knowledge, the crystal structure and photoluminescence properties of Eu-doped lanthanum aluminum oxynitride have not yet been reported.

cis-TaO_4N_2 octahedra have been assumed in the structure of perovskite-type $SrTaO_2N$ and $BaTaO_2N$ tantalum oxynitrides [19-22]. The large dielectric constant of these perovskites was considered to be related to the polarity induced in the distorted octahedra. Coexisting nitride and oxide ions together in a structure could change the coordination around lanthanum ions in the MP structure, which would result in splitting or distortion of the site occupied partially by Eu^{2+}. Therefore, a reduction in local symmetry may affect the emission of oxynitride phosphors.

In this study, Eu^{2+} doped products were prepared in MP-type lanthanum aluminum oxynitride and calcium aluminum oxide using aluminum glycine gel precursors followed by post-annealing of the calcined precursors. The luminescence properties of the product compounds are discussed in relation to the crystal structures refined by neutron diffraction analysis.

2. Experimental procedure

Aluminum acetylacetonate ($Al(acac)_3$, > 98.0%, Wako Chemicals Co.), lanthanum acetylacetonate hydrate ($La(acac)_3 \bullet nH_2O$ with n = 1.1, 99.9%, Wako Chemicals Co.) and europium acetylacetonate hydrate ($Eu(acac)_3 \bullet nH_2O$ with n = 1.8, 99.9%, Aldrich) were used as starting materials. The hydration numbers n, were estimated from thermogravimetric analysis. The starting powders were mixed in a La:Eu:Al molar ratio of 1-x:x:12 (x = 0-0.3) in anhydrous ethanol. Glycine (99.0%, Wako Pure Chemicals Co.) was added to the solution as a peptizer in an equimolar amount to the total cation content. The resultant solutions were heated on a hot plate under stirring to obtain gelatinous products. The gels were pre-fired in air at 500 °C for 1 h, and were then nitrided under an ammonia flow rate of 50 mL/min at 850 °C for 10 h. After grinding and mixing in an agate mortar, the products were post-annealed at 1700 °C in a gas pressure furnace for 3 h under a nitrogen gas pressure of

0.2 MPa. For the preparation of $Ca_{1-y}Eu_yAl_{12}O_{19}$ with y = 0.05, calcium acetylacetonate ($Ca(acac)_2 \bullet nH_2O$ with n = 0.5, 99.95%, Aldrich) was used instead of $La(acac)_3 \bullet nH_2O$. The pre-fired product was heated at 1400 °C for 12 h under a nitrogen flow rate of 100 mL/min in a horizontal tube furnace.

Crystalline phases were characterized using powder X-ray diffraction (XRD; Ultima IV, Rigaku) with monochromated Cu Kα radiation. Photoluminescence spectra were measured using a fluorescence spectrometer (FP-6500, Jasco) installed with a Xe lamp for excitation at 150 W. Emission spectra were measured in the 340-550 nm range with excitation at 254 nm. Excitation spectra were measured in the range of 230-400 nm with emission at 415 or 440 nm for $Ca_{1-y}Eu_yAl_{12}O_{19}$ or $La_{1-x}Eu_xAl(O,N)_{19}$, respectively. The oxygen and nitrogen contents were measured with an oxygen/nitrogen analyzer (EMGA-620W, Horiba) using Si_3N_4 and Y_2O_3 as references. Neutron diffraction data were collected for $La_{1-x}Eu_xAl(O,N)_{19}$ and $Ca_{1-y}Eu_yAl_{12}O_{19}$ with x = y = 0.03. Although Eu has a relatively large absorption cross section for neutron radiation, neutron diffraction data could be successfully measured because of the small doping concentration. Neutron diffraction measurements were performed at room temperature with a wavelength of 0.18240 nm using the Kinken powder diffractometer HERMES [23] installed at the JRR-3M reactor of the Japan Atomic Energy Agency (JAEA), Tokai, Japan. The Rietveld program RIETAN-2000

[24] was used for structural refinements. The refined crystal structure was visualized using the VESTA program [25]. X-ray absorption near edge structure (XANES) of the Eu L_{III}-edge was measured in the transmission mode at the BL-9C beam line of the Photon Factory at the High Energy Accelerator Research Organization (KEK), Tsukuba, with the storage ring operating at 2.5 GeV. For measurements, a small amount of the sample powder was sandwiched between Scotch tapes. $EuCl_2$, $EuCl_3$ and Eu_2O_3 were used as references.

3. Results and discussion

3.1. Photoluminescence properties of MP-type $La_{1-x}Eu_xAl_{12}(O,N)_{19}$.

The powders nitrided at 850 °C under ammonia flow were XRD amorphous. After post-annealing at 1700 °C for 3 h under a nitrogen gas pressure of 0.2 MPa, pure MP-type products were obtained for the entire $La_{1-x}Eu_x$ range prepared in this study, as shown in Fig. 1. The 008 diffraction line and related diffractions such as 203 and 206 were slightly shifted toward higher 2θ angle with increasing x. However, the peak positions for the hk0 planes did not change significantly among the products. The hexagonal lattice parameters were a = 0.5569(2) nm and c = 2.205(2) nm for $LaAl_{12}(O,N)_{19}$ without Eu doping, which were comparable to the reported values of a = 0.5570 nm and c = 2.203 nm for $LaAl_{12}O_{18}N$ [18]. They were decreased along with Eu doping to a = 0.5565(1) nm and c = 2.199(1) nm for 30

at% Eu-doped oxynitride (see Table S1 in supporting information). Europium aluminum oxide was also reported to crystallize in the MP structure with a composition of $EuAl_{12}O_{19}$, which has hexagonal lattice parameters of *a* = 0.5568 nm and *c* = 2.201 nm [26]. Therefore, Eu doping had a significant influence on the *c*-axis lattice parameter of the MP structure, but not on the *a*-axis. The oxygen and nitrogen content of the product without Eu doping was analyzed to be 38.8(10) wt% for O and 0.61(5) wt% for N, where the theoretical values were 37.8 wt% for O and 1.8 wt% for N in $LaAl_{12}O_{18}N$. The less nitrogen observed may be caused by only the partial decomposition of the sample in the analysis, so that the whole nitrogen was not released due to the high stability of aluminum oxynitride. The oxynitride without Eu doping was expected to have O/N ratio of 18:1, in order to keep charge neutrality in MP structure. The Eu-doped products prepared in this study also had nitrogen contents of approximately 0.5 wt% as summarized in Table S1 in SI.

Eu-doped lanthanum aluminum oxynitrides exhibited broad blue emission at 440 nm with a shoulder peak at 464 nm under excitation at 254 nm, as shown in Fig. 2(a). No characteristic sharp peaks due to Eu^{3+} ions were observed, which confirms the presence of only Eu^{2+} ions in the phosphors. The Eu^{2+} was supported by a single absorption peak at 6972 eV in the XANES spectra for the Eu L_{III}-edge. The former wavelength is comparable to that reported for MP-type $LaMgAl_{11}O_{19}:Eu^{2+}$ [11]; however, there is a characteristic shoulder

peak at 464 nm in Eu-doped $LaAl_{12}(O,N)_{19}$. The products exhibited broad excitation spectra between 250 and 360 nm for the emission at 440 nm, as depicted in Fig. 2(b). XRD patterns indicated no impurities were present in the products, however trace amount of $LaAlO_3$ (1 wt%) was observed in neutron diffraction pattern of $La_{0.97}Eu_{0.03}Al_{12}(O,N)_{19}$ due to the higher detectability as shown in Fig. 4. Eu doped $LaAlO_3$ have been reported to exhibit multiple emission peaks at 440, 515, 592 and 618 nm [27]. No emission peaks at 515, 592 and 618 nm were observed in the products as shown in Fig. 2(a). Therefore the two emission peaks could be attributed to only the oxynitride. The reason for the emission is discussed in the next section with the results of the structure refinement. The highest emission and excitation intensity were observed for the 5 at% Eu-doped product. At doping concentrations above 5 at%, the intensity decreased due to concentration quenching.

Single phase $Ca_{0.95}Eu_{0.05}Al_{12}O_{19}$ was obtained after heating at 1400 °C for 12 h (see Fig. S1 in SI), which exhibited a single broad emission at 415 nm, as shown in Fig. 3. The emission wavelength was shorter than that for Eu-doped $LaAl_{12}(O,N)_{19}$. It is believed that the long wavelength emission is attributed to covalent bond character and a large crystal field splitting effect on Eu^{2+} 5d band [28]. The emission wavelength was red-shifted for (Ca,Y)-α-SiAlON:Eu^{2+} by the substitution of smaller Y^{3+} (r_{Y3+} = 0.110 nm, for C.N. = 7) with Ca^{2+} (r_{Ca2+} = 0.120 nm, for C.N. = 7) [29], due to changes in the crystal field splitting of

Eu^{2+} [30]. The ionic radii of La^{3+} is comparable with Ca^{2+}; r_{La3+} = 0.150 nm and r_{Ca2+} = 0.148 nm for C.N. = 12 [29]. The present red-shift of the emission peak wavelength may be caused by the introduction of nitride ions to increase the covalent character. In the next section, the crystal structure of MP-type Eu-doped $LaAl_{12}(O,N)_{19}$ is refined to elucidate the origin of the emission shoulder peak observed for the oxynitride.

3.2. Eu site splitting in MP-type oxynitride host structure

A small amount of Eu-doped product was used for neutron diffraction measurements due to a large neutron absorption cross section of Eu. For both 3 at% doped lanthanum aluminum oxynitride and calcium aluminum oxide, sufficient diffraction patterns for the structural refinement were observed as shown in Fig. 4 and Fig. S2. The crystal structure of $La_{0.97}Eu_{0.03}Al_{12}(O,N)_{19}$ was refined in the MP structure starting from the crystallographic parameters of $CaAl_{12}O_{19}$ [13]. Structure refinement as aluminum oxide not as oxynitride did not converge into reasonable structural parameters. The oxygen/nitrogen ratio was fixed at 0.95/0.05, as expected from the stoichiometric composition. The final refined parameters showed an unusually large isotropic displacement (U_{iso}) of $0.0234(13)\times10^{-2}$ nm^2 on the 2*d* site occupied by 97% La and 3% Eu, which resulted in inferior fitting values of R_{wp} = 6.84%, R_e = 3.25% and S = 2.11 in the preliminary refinement.

Lanthanum ions in inorganic compounds (oxides, nitrides and oxynitrides) usually have an isotropic displacement parameter between 0.006-0.014×10^{-2} nm^2 [31-33]. The anomalously large isotropic displacement parameter on the lanthanum site may be attributed to site splitting. Lanthanum site splitting has been reported in the MP-type lanthanum aluminate with cation and anion vacancies ($La_{0.85}Al_{11.5}O_{18.5}$) [31], but is not evident in stoichiometric $AEAl_{12}O_{19}$ (AE = Ca or Sr) without vacancies [13,14]. The lanthanum site splitting from the original 2*d* site to 2*d* and 6*h* sites was applied for further refinement. The final refined parameters from the Rietveld refinement are summarized in Table 1. The observed, calculated and difference neutron diffraction profiles for $La_{0.97}Eu_{0.03}Al_{12}(O,N)_{19}$ are shown in Fig. 4. The refinement was improved to R_{wp} = 5.97%, R_e = 3.22% and S = 1.85 when site splitting was applied. The isotropic displacement on the lanthanum sites was refined to a reasonable value of 0.0028(9)×10^{-2} nm^2. Preferential occupation of the europium or nitride ions on lanthanum sites (2*d* and 6*h*) or anion sites (6*h*, 12*k*, 12*k*, 4*e*, 4*f*), respectively, was not distinguished. The crystal structure of $Ca_{0.97}Eu_{0.03}Al_{12}O_{19}$ was also refined in the MP structure. The refinement showed a good fit with the structural model without calcium site splitting, as reported in Refs [13,14] (see Fig. S2 and Table S2 in SI). The refined isotropic displacement on the calcium site is 0.010(2)×10^{-2} nm^2, which is comparable to that reported for MP-type $CaAl_{12}O_{19}$ [13] and other oxides [34,35]. The bond lengths around lanthanum

and calcium sites are summarized in Table 2. The atomic arrangements around the lanthanum and calcium sites in the MP-type oxynitride and oxide were visualized using the VESTA program [25] and are shown in Fig. 5. The original 2*d* sites (RE1 and CA1) are in similar coordination environments to each other in the respective crystal structures. The bond length of La-N is approximately 0.265 nm in LaN and longer than that of La-O (0.258 nm) in La_2O_3 [36,37]. Some of La ions are shifted in their position from the 2*d* site to the 6*h* site so as to be apart from the introduced nitride ion, which results in lanthanum site splitting in the oxynitride structure.

The emission peak splitting that was observed can be attributed to Eu site splitting into the 2*d* and 6*h* sites. The 6*h* site has lower symmetry than the 2*d* site and its coordination number may be decreased from 12 to 10, as shown in Fig. 5. Lower symmetry and smaller coordination number results in an increase in the crystal field splitting effect on Eu^{2+}, which results in the red-shift emission. The emission peak at 440 nm and the shoulder at 460 nm may be caused by emission from Eu^{2+} on the 2*d* and 6*h* sites, respectively.

4. Conclusion

Eu-doped lanthanum aluminum oxynitride with MP structure were prepared by nitridation of oxide precursors obtained from aluminum glycine gel and subsequent

post-annealing at 1700 °C for 3 h under 0.2 MPa N_2. The product exhibited a broad blue emission at 440 nm with a shoulder peak at 464 nm under excitation at 254 nm. The highest emission intensity was observed at 5 at% of Eu doping. It showed a wide excitation spectrum at 250-380 nm with emission at 440 nm. The calcium aluminum oxide had a single emission peak at 415 nm. The longer emission and wider excitation wavelength observed for the aluminum oxynitride than that for the oxide were related to an increase in the covalency around Eu^{2+} due to the presence of nitride ions. Structural refinement using neutron diffraction showed the lanthanum site occupied by Eu^{2+} is split into 2*d* and 6*h* sites at the intermediate layer in the MP-type aluminum oxynitride. The shoulder emission peak in the emission spectrum of the oxynitride is not directly related to two kinds of anions, but to the Eu^{2+} site splitting induced by the two kinds of anions.

Acknowledgement

Neutron diffraction measurements were performed under the approval of 10750 in the JRR-3M reactor at JAEA. XANES measurements were conducted under the approval of the Photon Factory Advisory Committee (Proposal No. 2010G024). This research was partly supported by the Global COE Program (Project No. B01: “Catalysis as the Basis for Innovation in Materials Science”) and a Grant-in-Aid for Scientific Research on Priority

Areas (No. 22015001) from the Ministry of Education, Culture, Sports, Science and Technology of Japan.

References

[1] T. Justel, H. Nikol, C. Ronda, Angew. Chem. Int. Ed. 37 (1998) 3084-3103

[2] R.J. Xie, N. Hirosaki, M. Mitomo, K. Sakuma, N. Kimura, Appl. Phys. Lett. 89 (2006) 241103

[3] H. Luo, J.K. Kim, E.F. Schubert, J. Cho, C. Sone, Y. Park, Appl. Phys. Lett. 86 (2005) 243505.

[4] X. Piao, T. Horikawa, H. Hanazawa, K. Machida, Appl. Phys. Lett. 88 (2006) 161908.

[5] R.J. Xie, N. Hirosaki, Sci. Technol. Adv. Mater. 8 (2007) 588–600.

[6] J. Jeong, M. Jayasimhadri, H.S. Lee, K. Jang, S.S. Yi, J.H. Jeong, C. Kim, Physica B 404 (2009) 2016-2019.

[7] N. Guo, H. You, Y. Song, M. Yang, K. Liu, Y. Zheng, Y. Huang, H. Zhang, J. Mater. Chem. 20 (2010) 9061-9067.

[8] B. Lei, L. Sha, H. Zhang, Y. Liu, S. Man, S. Yue, Solid State Sci. 12 (2010) 2177-2181.

[9] X.W. Zhu, Y. Masubuchi, T. Motohashi, S. Kikkawa, J. Alloys Compd. 489 (2010) 157-161.

[10] S. Kikkawa, N. Hatta, T. Takeda, J. Am. Ceram. Soc. 91 (2008) 924-928.

[11] A.L.N. Stevels, A.D.M. Schrama-de Pauw, J. Electrochem. Soc. 123 (1976) 691-697.

[12] S. R. Jansen, J. W. de Haan, L. J. M van de Ven, R. Hanssen, H. T. Hintzen, R.

Metselaar, Chem. Mater. 9 (1997) 1516-1523.

[13] A. Utsunomiya, K. Tanaka, H. Morikawa, F. Marumo, H. Kojima, J. Solid State Chem. 75 (1988) 197-200.

[14] A.J. Lindop, C. Matthews, D.W. Goodwin, Acta Crystallogr. B 31 (1975) 2940-2941.

[15] S.R. Jansen, J.M. Migchels, H.T. Hintzen, R. Metselaar, J. Electrochem. Soc. 146 (1999) 800-806.

[16] T.E. Warner, D.J. Fray, A. Davies, Solid State Ionics 92 (1996) 99-101.

[17] X.H. Wang, A.M. Lejus, D. Vivien, J. Am. Ceram. Soc. 73 (1990) 770-774.

[18] X.W. Wang, A.M. Lejus, D. Vivien, R. Collongues, Mater. Res. Bull. 23 (1988) 43-49.

[19] S.G. Ebbinghaus, H.P. Abicht, R. Dronskowski, T. Muller, A. Reller, A. Weidenkaff, Prog. Solid State Chem. 37 (2009) 173-205.

[20] B. Ravel, Y-I. Kim, P.M. Woodward, C.M. Fang, Phys. Rev. B 73 (2006) 184121.

[21] Y. Zhang, T. Motohashi, Y. Masubuchi, S. Kikkawa, J. Ceram. Soc. Jpn. 119 (2011) 581-586.

[22] M. Yang, J. Oro-Sole, J. A. Rodgers, A. B. Jorge, A. Fuertes, J. P. Attfield, Nat Chem. 3 (2011) 47-52.

[23] K. Ohoyama, T. Kanouchi, K. Nemoto, M. Ohashi, T. Kajitani, Y. Yamaguchi, Jpn. J. Appl. Phys. 37 (1998) 3319-3326.

[24] F. Izumi, T. Ikeda, Mater. Sci. Forum 321-324 (2000) 198-203.

[25] K. Momma, F. Izumi, J. Appl. Crystallogr. 41 (2008) 653-658.

[26] H.T. Hintzen, R. Hanssen, S.R. Jansen, R. Metselaar, J. Solid State Chem. 142 (1999) 48-50.

[27] Z. Mao, D. Wang, Q. Lu, W. Yu, Z. Yuan, Chem. Commun. (2009) 346-348.

[28] P. Dorenbos, J. Lumin. 104 (2003) 239-260.

[29] R.D. Shannon, Acta Crystallogr. A 32 (1976) 751-767.

[30] K. Sakuma, N. Hirosaki, R.J. Xie, Y. Yamamoto, T. Suehiro, Mater. Lett. 61 (2007) 547-550

[31] M. Gasperin, M.C. Saine, A. Kahn, F. Laville, A.M. Lejus, J. Solid State Chem. 54 (1984) 61-69.

[32] M. Yashima, M. Saito, H. Nakano, T. Takata, K. Ogisu, K. Domen, Chem. Comm. 46 (2010) 4704-4706.

[33] D. Logvinovich, S.G. Ebbinghaus, A. Reller, I. Marozau, D. Ferri, A. Weidenkaff, Z. Anorg. Allg. Chem. 636 (2010) 905-912.

[34] H.M. Palmer, A. Snedden, A.J. Wright, C. Greaves, Chem. Mater. 18 (2006) 1130-1133.

[35] D.W. Goodwin, A.J. Lindop, Acta Crystallogr. B 26 (1970) 1230-1235.

[36] W. Klemm, G. Winkelmann, Z. Anorg. Allg. Chem. 288 (1956) 87-90.

[37] W.C. Koehler, E.O. Wollen, Acta Crystallogr. 6 (1953) 741-742.

Table 1

Refined structural parameters for $La_{0.97}Eu_{0.03}Al_{12}(O,N)_{19}$ at room temperature.

Atom	site	*g*	*x*	*Y*	*z*	U_{iso} / $\times 10^{-2}$ nm^2 (=Å^2)
RE1	2*d*	0.55(1)	2/3	1/3	1/4	0.0028(9)
RE2	6*h*	0.15(1)	0.7117(9)	= 2*x*	1/4	0.0028(9)
Al1	2*a*	1	0	0	0	0.0013(11)
Al2	4*f*	1	1/3	2/3	0.0276(2)	0.0069(12)
Al3	4*f*	1	1/3	2/3	0.1898(2)	0.0015(13)
Al4	12*k*	1	0.8315(3)	= 2*x*	0.1077(1)	0.0046(5)
Al5	4*e*	0.5	0	0	0.2358(4)	0.006(2)
ON1	6*h*	1	0.1810(3)	= 2*x*	1/4	0.0096(6)
ON2	12*k*	1	0.1563(2)	= 2*x*	0.0521(1)	0.0036(4)
ON3	12*k*	1	0.5041(2)	= 2*x*	0.1501(1)	0.0051(4)
ON4	4*e*	1	0	0	0.1485(1)	0.0045(9)
ON5	4*f*	1	2/3	1/3	0.0556(1)	0.0017(6)

R_{wp} = 5.97%, R_p = 4.50%, R_e = 3.22%, S = 1.85. S.G.: $P6_3/mmc$,

a = 0.55686(1) nm, c = 2.20524(3) nm. RE = 0.97La/0.03Eu, ON = 0.95O/0.05N

Table 2

Selected bond lengths (nm) for $La_{0.97}Eu_{0.03}Al_{12}(O,N)_{19}$ and $Ca_{0.97}Eu_{0.03}Al_{12}O_{19}$.

$La_{0.97}Eu_{0.03}Al_{12}(O,N)_{19}$			
RE1 (2*d*)	ON1 (6*h*)	× 6	0.2788(2)
	ON3 (12*k*)	× 6	0.27026(14)
RE2 (6*h*)	ON1 (6*h*)	× 2	0.2442(2)
	ON1 (6*h*)	× 2	0.2799(2)
	ON1 (6*h*)	× 2	0.3172(2)
	ON3 (12*k*)	× 4	0.2611(2)
	ON3 (12*k*)	× 2	0.2969(2)
$Ca_{0.97}Eu_{0.03}Al_{12}O_{19}$			
CA1 (2*d*)	O1 (6*h*)	× 6	0.2783(2)
	O3 (12*k*)	× 6	0.27162(13)

Figure captions

Figure 1 XRD patterns for MP-type $La_{1-x}Eu_xAl_{12}(O,N)_{19}$ with various *x*; (a) *x* = 0, (b) *x* = 0.01, (c) *x* = 0.03, (d) *x* = 0.05, (e) *x* = 0.07, (f) *x* = 0.10, (g) *x* = 0.20, and (h) *x* = 0.30.

Figure 2 (a) Emission and (b) excitation spectra for MP-type $La_{1-x}Eu_xAl_{12}(O,N)_{19}$. Emission spectra were measured under excitation at 254 nm and excitation spectra were monitored at 440 nm.

Figure 3 Emission and excitation spectra for MP-type $La_{0.95}Eu_{0.05}Al_{12}(O,N)_{19}$ (solid lines) and $Ca_{0.95}Eu_{0.05}Al_{12}O_{19}$ (broken lines). Emission spectra were measured under excitation at 254 nm and excitation spectra were monitored at 440 and 415 nm for $La_{0.95}Eu_{0.05}Al_{12}(O,N)_{19}$ and $Ca_{0.95}Eu_{0.05}Al_{12}O_{19}$, respectively.

Figure 4 Observed (+), calculated (solid line) and difference powder neutron diffraction profiles for MP-type $La_{0.97}Eu_{0.03}Al_{12}(O,N)_{19}$. Upper vertical bars indicate the positions of Bragg reflections for the MP phase and the lower bars indicate those for $LaAlO_3$ (1 wt%).

Figure 5 Atomic arrangement around the lanthanum and calcium sites in MP-type (a,c)

$La_{0.97}Eu_{0.03}Al_{12}(O,N)_{19}$, and (b,d) $Ca_{0.97}Eu_{0.03}Al_{12}O_{19}$. These structures were visualized with the VESTA program [24] using the refined structural parameters represented in Table 1 and S2. The structures in (c) and (d) are viewed along the c-axis.

Figure 1

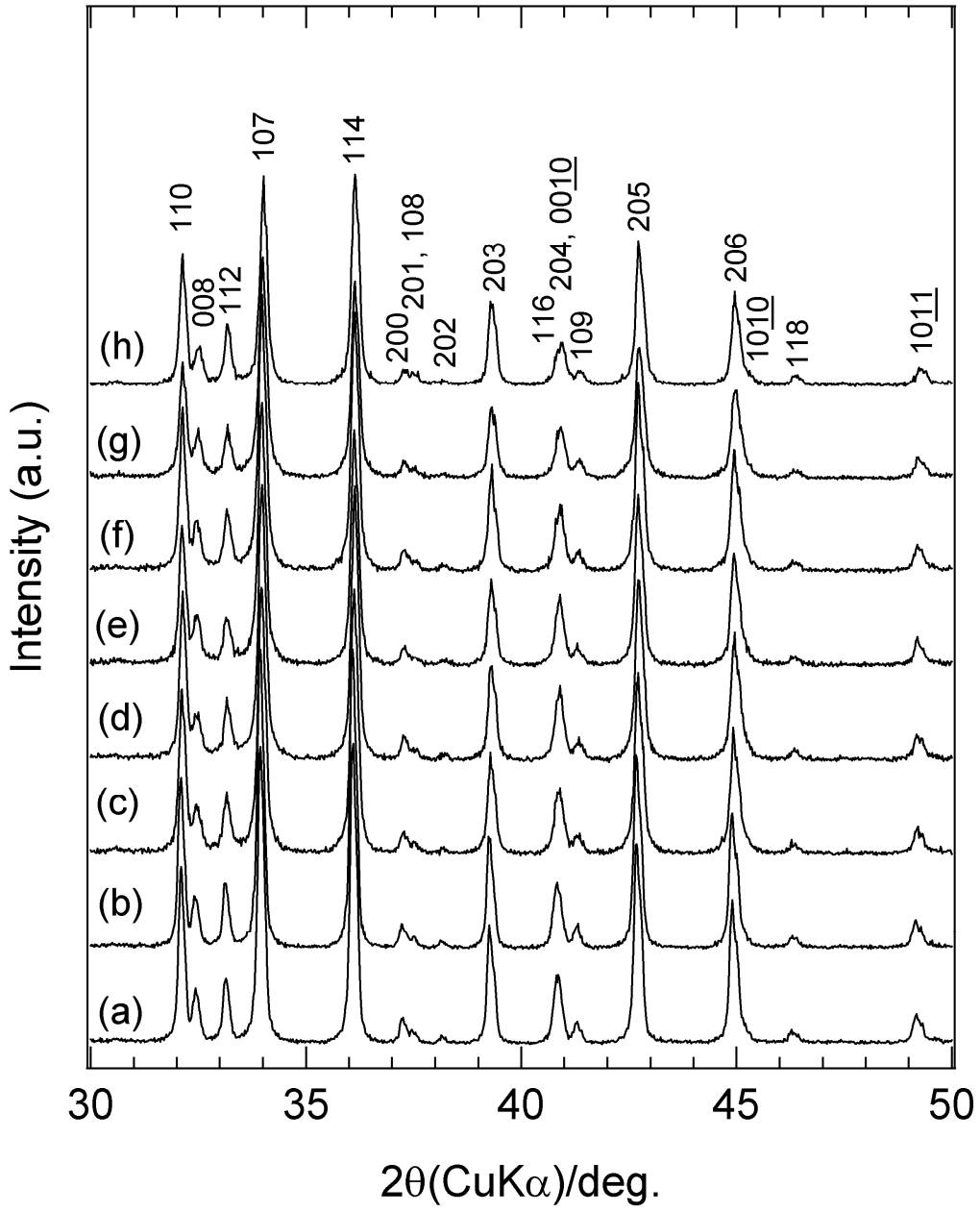

Figure 1 XRD patterns for MP-type $La_{1-x}Eu_xAl_{12}(O,N)_{19}$ with various x; (a) x = 0, (b) x = 0.01, (c) x = 0.03, (d) x = 0.05, (e) x = 0.07, (f) x = 0.10, (g) x = 0.20, and (h) x = 0.30.

Figure 2

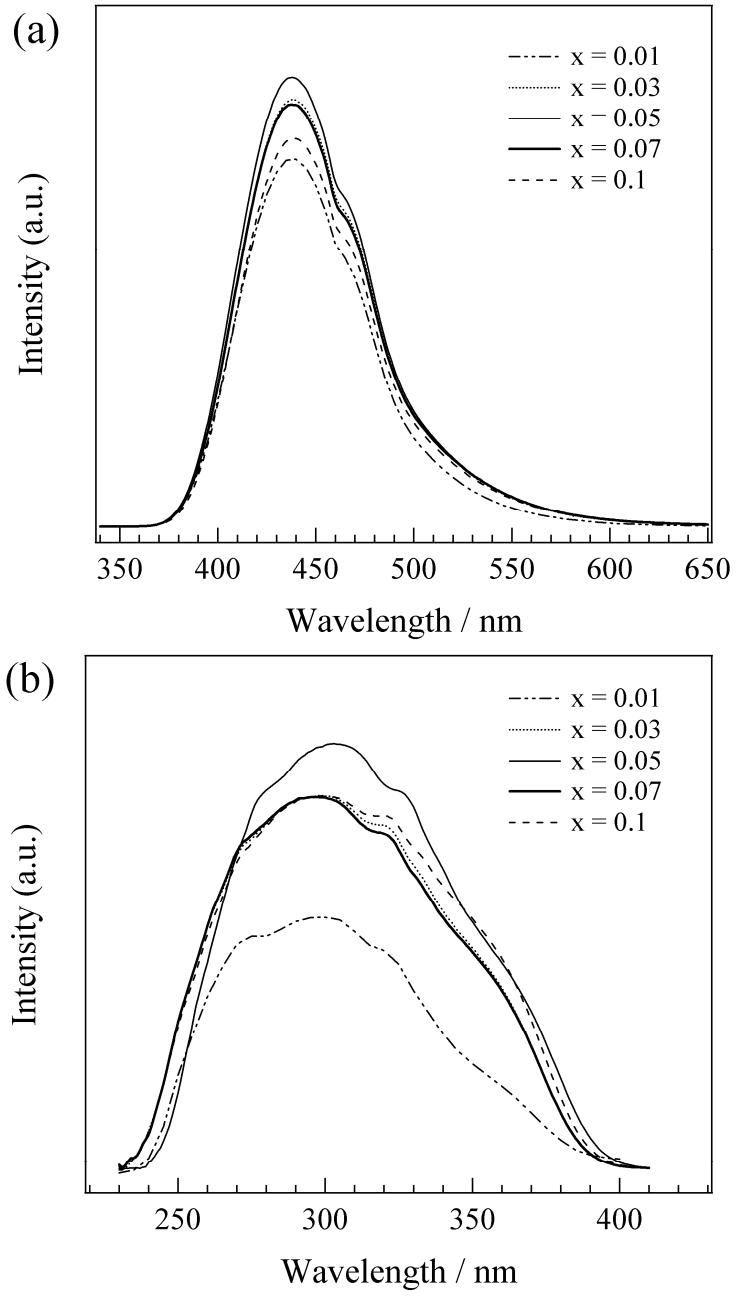

Figure 2 (a) Emission and (b) excitation spectra for MP-type $La_{1-x}Eu_xAl_{12}(O,N)_{19}$. Emission spectra were measured under excitation at 254 nm and excitation spectra were monitored at 440 nm.

Figure 3

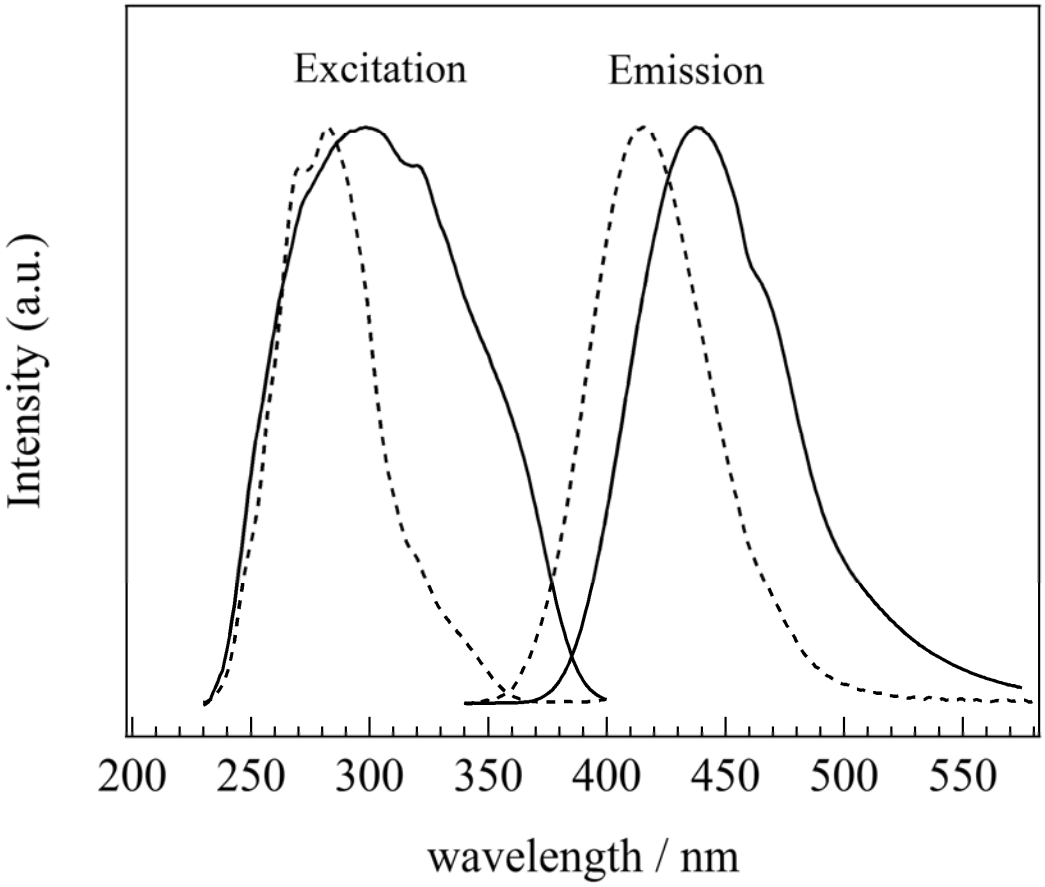

Figure 3 Emission and excitation spectra for MP-type $La_{0.95}Eu_{0.05}Al_{12}(O,N)_{19}$ (solid lines) and $Ca_{0.95}Eu_{0.05}Al_{12}O_{19}$ (broken lines). Emission spectra were measured under excitation at 254 nm and excitation spectra were monitored at 440 and 415 nm for $La_{0.95}Eu_{0.05}Al_{12}(O,N)_{19}$ and $Ca_{0.95}Eu_{0.05}Al_{12}O_{19}$, respectively.

Figure 4

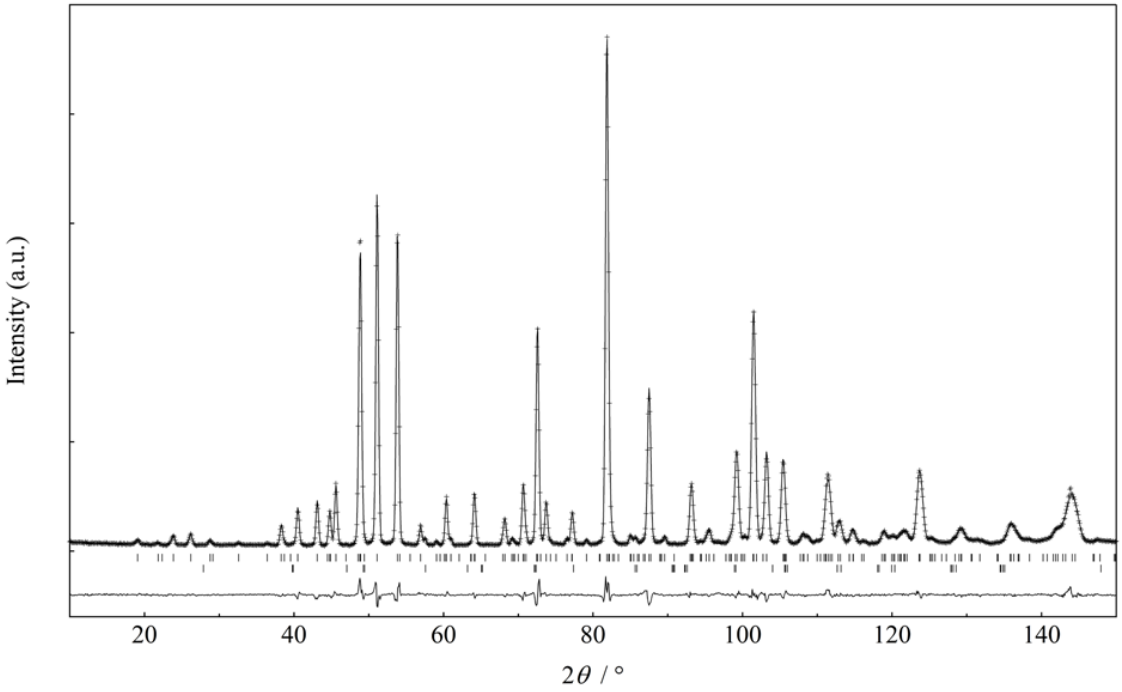

Figure 4 Observed (+), calculated (solid line) and difference powder neutron diffraction profiles for MP-type $La_{0.97}Eu_{0.03}Al_{12}(O,N)_{19}$. Upper vertical bars indicate the positions of Bragg reflections for the MP phase and the lower bars indicate those for $LaAlO_3$ (1 wt%).

Figure 5

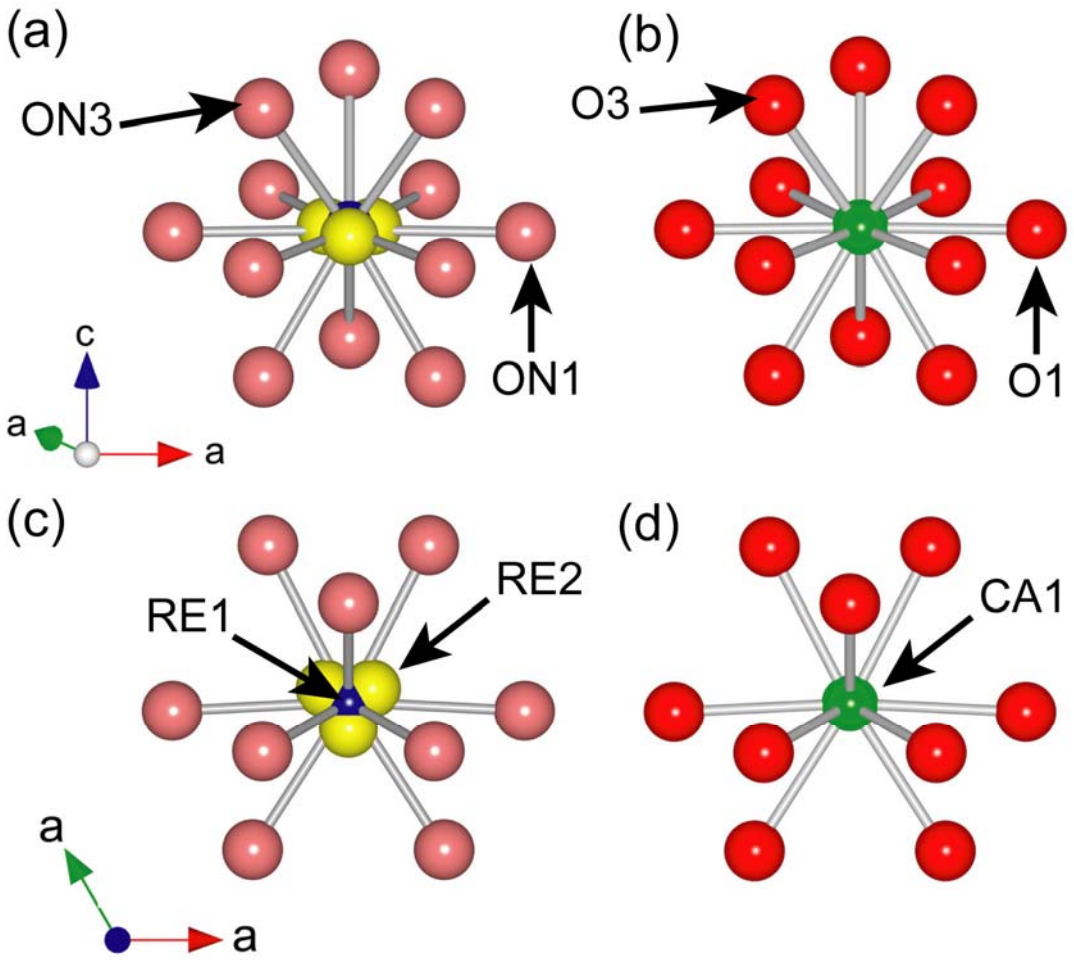

Figure 5 Atomic arrangement around the lanthanum and calcium sites in MP-type (a,c) $La_{0.97}Eu_{0.03}Al_{12}(O,N)_{19}$, and (b,d) $Ca_{0.97}Eu_{0.03}Al_{12}O_{19}$. These structures were visualized with the VESTA program [24] using the refined structural parameters represented in Table 1 and S2. The structures in (c) and (d) are viewed along the c-axis.